Title

Spectroscopic Characterization of an Eight-Iron Nitrogenase Cofactor Precursor that Lacks the "9th Sulfur"

Permalink

https://escholarship.org/uc/item/35g4z1p4

Journal

Angewandte Chemie International Edition, 58(41)

ISSN

1433-7851

Authors

Jasniewski, Andrew J
Wilcoxen, Jarett
Tanifuji, Kazuki
et al.

Publication Date

2019-10-07

DOI

10.1002/anie.201907593

Peer reviewed

Spectroscopic Characterization of an Eight-Iron Nitrogenase Cofactor Precursor That Lacks the "9th Sulfur"

Andrew J. Jasniewski[+,][a], **Jarett Wilcoxen**[+,][b], **Kazuki Tanifuji**[+,][a], **Britt Hedman**[c], **Keith O. Hodgson**[c],[d], **R. David Britt**[b], **Yilin Hu**[a], **Markus W. Ribbe**[a],[e]

[a]Department of Molecular Biology & Biochemistry, University of California, Irvine, Irvine, CA 92697-3900 (USA)

[b]Department of Chemistry, University of California, Davis, Davis, CA 95616 (USA)

[c]Stanford Synchrotron Radiation Lightsource, SLAC National Accelerator Laboratory, Stanford University, Menlo Park, CA 94025 (USA)

[d]Department of Chemistry, Stanford University, Stanford, CA 94305 (USA)

[e]Department Chemistry, University of California, Irvine, Irvine, CA 92697-2025 (USA)

Abstract

Nitrogenase catalyzes the reduction of N_2 to NH_4^+ at its cofactor site. Designated the M-cluster, this [MoFe$_7$S$_9$C(R-homocitrate)] cofactor is synthesized via transformation of a [Fe$_4$S$_4$] cluster pair into an [Fe$_8$S$_9$C] precursor (designated the L-cluster) prior to insertion of Mo and homocitrate. Here we report the characterization of an eight-iron cofactor precursor (designated the L*-cluster), which is proposed to have a composition of [Fe$_8$S$_8$C] and lack the "9th sulfur" in the belt region of the L-cluster. Our X-ray absorption and electron spin echo envelope modulation analyses strongly suggest that the L*-cluster represents a structural homolog to the L-cluster except for the missing belt sulfur. The absence of a belt sulfur from the L*-cluster may prove beneficial for labeling the catalytically important belt region, which could in turn facilitate investigations into the reaction mechanism of nitrogenase.

Graphical Abstract

This work reports the spectroscopic characterization of an Fe-only nitrogenase cofactor precursor (designated L*-cluster), which is proposed to have a composition of [Fe$_8$S$_9$C] and lack the "9th sulfur" in the belt region. The lack of a belt sulfur may prove beneficial for labelling this position for mechanistic studies of nitrogenase.

yilinh@uci.edu. mribbe@uci.edu. rdbritt@ucdavis.edu. hedman@slac.stanford.edu. hodgsonk@stanford.edu.

[+]These authors contributed equally.
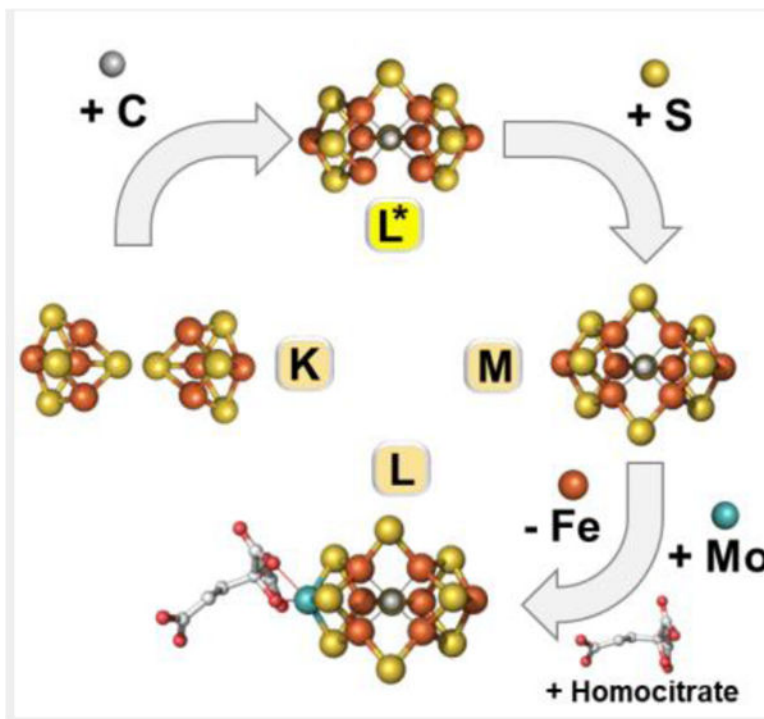
Introduction

Nitrogenase catalyzes the conversion of atmospheric nitrogen to ammonia at ambient temperature and pressure, thereby providing a reduced nitrogen source required by all life forms on Earth for the generation of fundamental cellular building blocks.[1–4] Substrate reduction by nitrogenase is a multi-electron process that is carried out at its cofactor site. Known as the M-cluster (or FeMoco), this complex metallocofactor has a composition of [MoFe$_7$S$_9$C(R-homocitrate)] and features MoFe$_3$S$_3$ and Fe$_4$S$_3$ subcubanes that are ligated by three "belt" μ_2-sulfides (S^{2-}) and an interstitial μ_6-carbide (C^{4-}) (Figure S1a).[5,6] Situated within the α-subunit of the catalytic component (designated the MoFe protein, or NifDK) of the Mo-dependent nitrogenase of the diazotrophic organism, *Azotobacter vinelandii*, the M-cluster receives electrons from the reductase component (designated the Fe protein, or NifH) of Mo-nitrogenase, which passes electrons in an ATP-dependent process from its [Fe$_4$S$_4$] cluster, via a so-called P-cluster ([Fe$_8$S$_7$]) at the α/β-subunit interface of NifDK, to the M-cluster to enable substrate reduction.

Considerable effort has gone into investigations of the biosynthesis of the M-cluster,[7–9] as a better understanding of this process could shed important light on the structure-function relationship of nitrogenase. The bioassembly of M-cluster involves several *nif*-encoded proteins, starting at NifS/U and terminating at NifDK, and the pathway involves a number of co-substrates that facilitate the transformation of clusters (Figure S1a).[9] Of the various

biosynthetic events, the most dramatic occurs on NifB, a radical *S*-adenosyl-*L*-methionine (SAM) enzyme that is believed to catalyze the conversion of a $[Fe_4S_4]$ cluster pair (designated the K-cluster) to an $[Fe_8S_9C]$ cluster (designated the L-cluster) concomitant with radical SAM-dependent insertion of an interstitial carbide (Figure 1a).[10–16] Representing both a precursor and an all-Fe structural homolog of the M-cluster, the L-cluster is then transferred to NifEN, where it is matured into an M-cluster upon substitution of a terminal Fe with Mo and homocitrate by NifH.[17–19] Subsequently, the M-cluster is transferred to its target binding site in apo-NifDK, resulting in a holo-NifDK that is competent in nitrogenase catalysis.

Previously, we have confirmed that a heterologously expressed homologue of NifB from *Methanosarcina acetivorans* (*Ma*NifB) indeed contains two FeS cluster species: the SAM-cluster (*i.e.*, a SAM-binding $[Fe_4S_4]$ cluster) and the K-cluster (*i.e.*, a pair of $[Fe_4S_4]$ clusters); further, we have demonstrated that upon reconstitution of its cluster species, *Ma*NifB can facilitate the K- to L-cluster conversion in the presence of SAM.[13,15,20] Such a process requires incorporation of an interstitial carbide and a "9th sulfur" to complete the stoichiometry of the L-cluster. While the source of carbide has been traced to the methyl group of SAM,[11,12] the origin of the "9th sulfur" has remained elusive. Recently, however, it was shown to be possible to reconstitute *Ma*NifB by synthetic $[Fe_4S_4]$ clusters. This procedure yielded a protein free of sulfur impurities introduced by the conventional $FeCl_3/Na_2S$ reconstitution procedure and thereby permitting the subsequent assessment of various sulfur compounds as the potential "9th sulfur" donor.[15] Not surprisingly, in the absence of a "9th sulfur" donor, the SAM-treated *Ma*NifB protein species cannot be used as an L-cluster source for the L- to M-cluster maturation and the subsequent activation of apo-NifDK by the matured M-cluster; however, the maturation activity can be restored when *Ma*NifB is incubated with SAM and sulfite (SO_3^2), pointing to sulfite as a source of the "9th sulfur" (Figure 1b). [15] Interestingly, although it is inactive in the maturation assay, *Ma*NifB treated with SAM but not sulfite exhibits the same, L-cluster-specific electron paramagnetic resonance (EPR) signal as that displayed by *Ma*NifB treated with both SAM and sulfite (Figure 1c).[15] Since the L-cluster-specific EPR signal is a marker for the formation of an all-Fe core of the nitrogenase cofactor, this observation suggests that the coupling and rearrangement of two $[Fe_4S_4]$ clusters into the core structure of the L-cluster has already occurred upon incubation with SAM, prior to the insertion of the "9th sulfur". Based on this observation, the inactive cluster species on the SAM-treated *Ma*NifB (designated the L*-cluster) is proposed to be an $[Fe_8S_8C]$ precursor of the nitrogenase cofactor, which lacks one of the belt μ_2-sulfide ligand and is ready to receive the "9th sulfur" from sulfite for the formation of an L-cluster (Figure 1a).[15]

Results and Discussion

To test our proposal that a "9th sulfur"-deplete form appears prior to the sulfur-replete form of the L-cluster, we first used CW and pulse electron paramagnetic resonance (EPR) techniques to monitor the biosynthetic events leading to the formation of the L*-cluster. Recently, CW and pulse EPR techniques were used as an effective spectroscopic handle for the analysis of the cluster-binding sites on NifB.[20,21] Combined with mutagenic and biochemical analyses, these spectroscopic studies have led to the successful identification of

nine Cys ligands—three per cluster—for the three [Fe_4S_4] clusters on *Ma*NifB, namely, the SAM-cluster and the two 4Fe modules of the K-cluster (designated the K1- and K2-cluster, respectively). Additionally, a fourth, nitrogen ligand (from a His residue) was assigned by three-pulse electron spin echo envelope modulation (3P-ESEEM) and two-dimensional hyperfine sub-level correlation (HYSCORE) experiments to the K1 cluster. Interestingly, the nitrogen coupling to the K1 cluster in *Ma*NifB—reflected by modulations to the electron spin echo from hyperfine and quadrupole couplings of a cluster-ligated ^{14}N nucleus—is lost upon incubation of *Ma*NifB with SAM and SO_3^{2-}, when the K1- and K2-modules were coupled into an L-cluster.[20] This observation suggests the utility of 3p-ESEEM in probing whether the cluster conversion has taken place on *Ma*NifB, with the loss of nitrogen ligation as a marker in this case.

Using our previous data as a standard for nitrogen ligation from a His ligand of *Ma*NifB, we examined the untreated, SAM-treated and SAM/SO_3^{2-}-treated *Ma*NifB (designated *Ma*NifB^{SAM+K}, *Ma*NifB^{SAM+L*} and *Ma*NifB^{SAM+L}, respectively; *see* Figure S1b for cluster compositions of these *Ma*NifB species) by 3P-ESEEM. As expected, the untreated sample, *Ma*NifB^{SAM+K}, shows deep modulations in the time domain of the ESEEM spectrum (Figure 2a) and the corresponding intensity between 0–6 MHz in the FFT (Figure 2b), indicating the presence of the nitrogen ligand in this sample. Upon SAM treatment in the absence or presence of SO_3^{2-}, however, the resulting *Ma*NifB^{SAM+L*} or *Ma*NifB^{SAM+L} sample no longer displays the deep modulations to the echo intensity (Figure 2a, b), suggesting a loss of nitrogen coupling to the L*- or L-cluster. Together, these results point to a structural rearrangement upon conversion of the K- to L*-cluster, which is accompanied by a change in the ligation of the cluster species to the protein scaffold.

X-ray absorption near edge structure (XANES) analysis was then carried out to provide insights into the electronic environment and symmetry of the Fe atoms of *Ma*NifB-bound clusters. As measured, the Fe K-edge energies are 7117.9, 7118.0 and 7118.1 eV for the cluster species in *Ma*NifB^{SAM+K}, *Ma*NifB^{SAM+L*} and *Ma*NifB^{SAM+L}, respectively (Figure S2), similar to those reported for the FeS-clusters in the Ni-Fe hydrogenase (7118 to 7119 eV),[22] indicating that the Fe centers in the *Ma*NifB species are all in a similar sulfur ligand environment. To circumvent complications originating from the presence of more than one cluster species on *Ma*NifB, data collected on *Ma*NifB^{SAM}—the *Ma*NifB variant carrying only the SAM-cluster—were subtracted from those collected on *Ma*NifB^{SAM+K}, *Ma*NifB^{SAM+L*} and *Ma*NifB^{SAM+L}, respectively, to yield information on the pre-edge peaks in the XANES region of the *Ma*NifB-bound K-, L*- and L-clusters (designated *Ma*NifB-K, *Ma*NifB-L* and *Ma*NifB-L) (Table S1). Subsequent analysis of the area under the pre-edge peak, which originates from a dipole-forbidden 1s→3d transition that increases in intensity as the metal center is distorted away from centrosymmetry,[23–26] provided the first hint of a significant structural rearrangement upon the K- to L*-cluster transformation, as well as a notable structural similarity between the L*- and L-clusters (see Supplementary Discussion for an expanded discussion of the pre-edge analysis).

Examination of the smoothed second derivative of the pre-edge data further demonstrated the structural similarity between *Ma*NifB-L* and *Ma*NifB-L, and between *Ma*NifB-L*/L and NifEN-L (Figure 3a). As described earlier,[27] the pre-edge spectrum of NifEN-L

consists of at least two well-spaced peaks centered at ~7112.6 and ~7114.5 eV, which reflects the unusual geometry of the L-cluster (or cofactor core) that is intermediate between tetrahedral and trigonal pyramidal.[28] In comparison, the pre-edge spectrum of *Ma*NifB-K apparently consists of a single broad peak centered at ~7112.6 eV, which is typical of protein-bound FeS clusters with tetrahedral Fe site geometries.[29] The pre-edge spectra of *Ma*NifB-L* and *Ma*NifB-L, on the other hand, have one peak at ~7112.6 eV and a second peak emerging at ~7114.5 eV, although the second feature is weaker in both *Ma*NifB-L and *Ma*NifB-L* as compared to that in NifEN-L, particularly in the case of *Ma*NifB-L*. The reduced intensity of the second feature of *Ma*NifB-L than that of NifEN-L suggests an impact of protein environment on the spectral properties of the same cluster species; whereas the fact that this feature in *Ma*NifB-L* (albeit weaker) resembles that in *Ma*NifB-L provides further evidence that major structural rearrangement has already occurred upon transformation of the K-cluster into an L*-cluster, rendering it in a conformation highly similar to that of the L-cluster.

Extended X-ray absorption fine structure (EXAFS) analysis of the Fe K-edge was subsequently performed to provide structural information about the ligands bound to the Fe centers, as well as structural metrics, such as Fe–S and Fe•••Fe distances, of the clusters on *Ma*NifB. The Fourier transforms (FT) of the EXAFS data of all *Ma*NifB-bound clusters (Figure 3b) have an intense feature at R+ ~ 1.7 Å that is associated with the Fe–S scatterers of the primary coordination sphere, and additional less intense features at R+ > 2 Å that are associated with Fe•••Fe distances of the metallocofactors.

For *Ma*NifB-K, the best fit is 2.29 Å for the Fe–S distance, which corresponds to the FT peak at R+ ~ 1.7 Å; in addition, there is a FT peak at R+ ~ 2.5 Å beyond the primary sphere that is comprised of contributions from Fe•••Fe distances at 2.51 and 2.69 Å (Table 1). These values agree well with those found in FeS cubane structures and support the previous assignment of *Ma*NifB-K as a [Fe$_4$S$_4$] cluster pair.[15,20,30]

*Ma*NifB-L* and *Ma*NifB-L, on the other hand, have intense primary sphere FT peaks at R+ ~ 1.7 Å (Figure 3b, *solid line*) that originate from Fe–S contributions at 2.24 and 2.23 Å, respectively, both of which are shorter than those found in the K-cluster (Table 1). These distances appear to be unique to the NifB-bound cofactor species, as they are on the lower end of the range found for FeS clusters in general (2.2 to 2.4 Å),[30] and are slightly shorter than the previously reported Fe–S distances from the EXAFS analyses of NifEN-bound (2.28 Å)[28] and extracted (2.26 Å)[31] L-clusters, as well as the average Fe–S distance from the crystallographically characterized M-cluster on NifDK (~2.25 Å, PDB code 3U7Q).[6] The FT peak associated with the Fe•••Fe distances of *Ma*NifB-L* and *Ma*NifB-L changes to a more intense feature at R+ ~2.4 Å relative to that of *Ma*NifB-K (Figure 3b, *dotted line*). The best fits for the Fe•••Fe distances associated with this feature were 2.62 and 2.64 Å for *Ma*NifB-L* and *Ma*NifB-L, respectively, and these distances are similar to those reported for other FeS clusters (~2.65 Å).[27,30] In addition, both *Ma*NifB-L* and *Ma*NifB-L have an additional FT peak at R+ ~3 Å (Figure 3b, *dashed line*), which originates from an Fe•••Fe distance at ~3.70 Å (Table 1). This observation is important, as this Fe•••Fe distance is consistent with the long-range order characteristic of the cofactor structure and, therefore, is

a strong indication that the overall core structure of the cofactor is already in place in *Ma*NifB-L* and *Ma*NifB-L.[28,31]

While similar, the XAS spectra of *Ma*NifB-L* and *Ma*NifB-L are not identical to each other. The features of *Ma*NifB-L* in the FT at ~2.1 Å and in the k^3-weighted EXAFS data at k ~8.5 Å^{-1} are less pronounced than those of *Ma*NifB-L (Figure 3c, *blue vs. red*). It is not possible to directly interpret these subtle changes into a three-dimensional structure; however, since these spectroscopic features correspond to shorter Fe•••Fe distances, a decrease in the intensities of these features would suggest less strong scattering of the Fe atoms in *Ma*NifB-L* as compared to those in *Ma*NifB-L. Therefore, the L*-cluster may adopt a slightly more open conformation than the L-cluster, which would be consistent with the absence of a third μ_2-ligand in the belt region of the cluster. It is also important to note the similarity and dissimilarity between *Ma*NifB-L*/L and NifEN-L.[9,28,31] All three cluster species feature similar FT and k^3-weighted XAS spectra and fits, although NifEN-L has a much more intense FT peak at ~2.1 Å, as well as a well-defined beat at k~8.5 Å^{-1} in the EXAFS spectrum, both of which are associated with an Fe•••Fe distance at 2.64 Å (Figure 3c). Coupled with the contraction of the bond metrics observed for *Ma*NifB-L*/L, the difference in scattering for the corresponding spectra could indicate that the specific active site environments on NifB and NifEN structurally constrain the cluster in different ways to accommodate different cluster maturation events that occur on these two biosynthetic scaffolds, as well as the event of cluster transfer between the two scaffolds.

Conclusions

In summary, we have provided strong spectroscopic evidence for the appearance of a "9th sulfur"-deplete L*-cluster during the biosynthesis of the nitrogenase cofactor. Our results clearly show that the L*-cluster differs from the K-cluster in the addition of the interstitial carbide and the loss of the histidine ligand that coordinates the K-cluster. Moreover, the L*-cluster is clearly distinct from the L-cluster in lacking not only the '9th sulfur', but also the strong Fe-Fe interactions observed in the EXAFS analysis of the L-cluster, presumably due to a significantly more open cluster geometry of the L*-cluster compared to that of the L-cluster. The absence of a μ_2-belt sulfide from the L*-cluster is consistent with the labile nature of the belt region of the cofactor,[32,33] which may facilitate activation of the Fe sites coordinated by the belt sulfide(s) during catalysis. While the "vacant" site of the L*-cluster is likely occupied by a putative cysteine thiolate or H_2O ligand for the stabilization of the cofactor structure, it can be easily "reconstituted" upon treatment with sulfite. This feature could prove beneficial for labeling the catalytically important belt region of the nitrogenase cofactor, which could in turn facilitate investigations into the catalytic mechanism of nitrogenase.

Supplementary Material

Refer to Web version on PubMed Central for supplementary material.

Acknowledgements

References

[1]. Burgess BK, Lowe DJ, Chem. Rev 1996, 96, 2983. [PubMed: 11848849]

[2]. Howard JB, Rees DC, Chem. Rev 1996, 96, 2965. [PubMed: 11848848]

[3]. Hoffman BM, Lukoyanov D, Yang ZY, Dean DR, Seefeldt LC, Chem. Rev 2014, 114, 4041. [PubMed: 24467365]

[4]. Hoffman BM, Lukoyanov D, Dean DR, Seefeldt LC, Acc. Chem. Res 2013, 46, 587. [PubMed: 23289741]

[5]. Lancaster KM, Roemelt M, Ettenhuber P, Hu Y, Ribbe MW, Neese F, Bergmann U, DeBeer S, Science 2011, 334, 974. [PubMed: 22096198]

[6]. Spatzal T, Aksoyoglu M, Zhang L, Andrade SLA, Schleicher E, Weber S, Rees DC, Einsle O, Science 2011, 334, 940. [PubMed: 22096190]

[7]. Lee SC, Lo W, Holm RH, Chem. Rev 2014, 114, 3579. [PubMed: 24410527]

[8]. Ohki Y, Tatsumi K, Z. Anorg. Allg. Chem 2013, 639, 1340.

[9]. Ribbe MW, Hu Y, Hodgson KO, Hedman B, Chem. Rev 2014, 114, 4063. [PubMed: 24328215]

[10]. Wiig JA, Hu Y, Ribbe MW, Proc. Natl. Acad. Sci. U. S. A 2011, 108, 8623. [PubMed: 21551100]

[11]. Wiig JA, Hu Y, Lee CC, Ribbe MW, Science 2012, 337, 1672. [PubMed: 23019652]

[12]. Wiig JA, Lee CC, Hu Y, Ribbe MW, J. Am. Chem. Soc 2013, 135, 4982. [PubMed: 23514429]

[13]. Fay AW, Wiig JA, Lee CC, Hu Y, Proc. Natl. Acad. Sci. U. S. A 2015, 112, 14829. [PubMed: 26627238]

[14]. Hu Y, Ribbe MW, Curr. Opin. Chem. Biol 2016, 31, 188. [PubMed: 26969410]

[15]. Tanifuji K, Lee CC, Sickerman NS, Tatsumi K, Ohki Y, Hu Y, Ribbe MW, Nat. Chem 2018, 10, 568. [PubMed: 29662207]

[16]. Wiig JA, Hu Y, Ribbe MW, Nat. Commun 2015, 6, 8034. [PubMed: 26259825]

[17]. Kaiser JT, Hu Y, Wiig JA, Rees DC, Ribbe MW, Science 2011, 331, 91. [PubMed: 21212358]

[18]. Hu Y, Corbett MC, Fay AW, Webber JA, Hodgson KO, Hedman B, Ribbe MW, Proc. Natl. Acad. Sci. U. S. A 2006, 103, 17119. [PubMed: 17050696]

[19]. Hu Y, Corbett MC, Fay AW, Webber JA, Hodgson KO, Hedman B, Ribbe MW, Proc. Natl. Acad. Sci. U. S. A 2006, 103, 17125. [PubMed: 17062756]

[20]. Rettberg LA, Wilcoxen J, Lee CC, Stiebritz MT, Tanifuji K, Britt RD, Hu Y, Nat. Commun 2018, 9, 2824. [PubMed: 30026506]

[21]. Wilcoxen J, Arragain S, Scandurra AA, Jimenez-Vicente E, Echavarri-Erasun C, Pollmann S, Britt RD, Rubio LM, J. Am. Chem. Soc 2016, 138, 7468. [PubMed: 27268267]

[22]. Buhrke T, Löscher S, Lenz O, Schlodder E, Zebger I, Andersen LK, Hildebrandt P, Meyer-Klaucke W, Dau H, Friedrich B, Haumann M, J. Biol. Chem 2005, 280, 19488. [PubMed: 15764814]

[23]. Westre TE, Kennepohl P, DeWitt JG, Hedman B, Hodgson KO, Solomon EI, J. Am. Chem. Soc 1997, 119, 6297.

[24]. Sarangi R, Coord. Chem. Rev 2013, 257, 459. [PubMed: 23525635]

[25]. Roe AL, Schneider DJ, Mayer RJ, Pyrz JW, Widom J, Que L, J. Am. Chem. Soc 1984, 106, 1676.

[26]. Randall CR, Shu L, Chiou Y-M, Hagen KS, Ito M, Kitajima N, Lachicotte RJ, Zang Y, Que L, Inorg. Chem 1995, 34, 1036.

[27]. Corbett MC, Hu Y, Fay AW, Ribbe MW, Hedman B, Hodgson KO, Proc. Natl. Acad. Sci. U. S. A 2006, 103, 1238. [PubMed: 16423898]

[28]. Einsle O, Tezcan FA, Andrade SLA, Schmid B, Yoshida M, Howard JB, Rees DC, Science 2002, 297, 1696. [PubMed: 12215645]

[29]. Musgrave KB, Angove HC, Burgess BK, Hedman B, Hodgson KO, J. Am. Chem. Soc 1998, 120, 5325.

[30]. Tan LL, Holm RH, Lee SC, Polyhedron 2013, 58, 206. [PubMed: 24072952]

[31]. Fay AW, Blank MA, Lee CC, Hu Y, Hodgson KO, Hedman B, Ribbe MW, Angew. Chem. Int. Ed 2011, 50, 7787.

[32]. Spatzal T, Perez KA, Howard JB, Rees DC, Elife 2015, 4, e11620. [PubMed: 26673079]

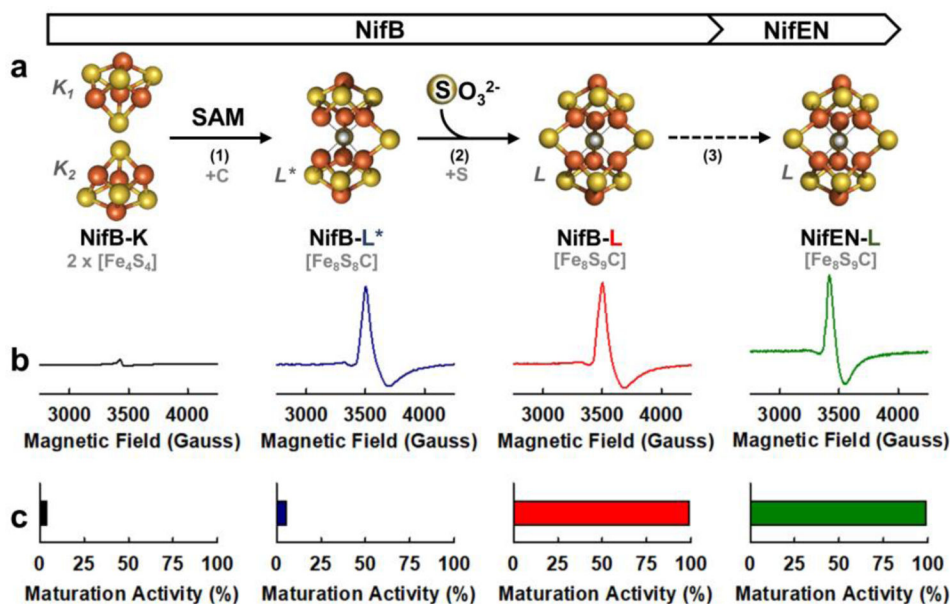[33]. Spatzal T, Perez KA, Einsle O, Howard JB, Rees DC, Science 2014, 345, 1620. [PubMed: 25258081]

Figure 1.
Biosynthesis of the nitrogenase cofactor precursors on NifB and NifEN. (**a**) Proposed assembly steps of the L-cluster species on NifB, including (1) formation of the putative L*-cluster via coupling/rearrangement of the two 4Fe modules (designated K1 and K2, respectively) of a K-cluster concomitant with SAM-dependent insertion of the interstitial carbide; (2) sulfite-dependent conversion of the putative L*-cluster into an L-cluster; and (3) transfer of the L-cluster from NifB to NifEN. Atoms are colored as follows: Fe, orange; S, yellow; C, grey. Note that one belt sulfur is behind the interstitial carbide and not visible in the cluster models as shown in a. The cluster composition is indicated in gray fonts. (**b**) Perpendicular-mode EPR spectra of the various precursor species of the cofactor. (**c**) Relative maturation activities using various precursors on NifB as a source to generate the M-cluster for the reconstitution/activation of NifDK. Data were taken from refs. 13 and 15.
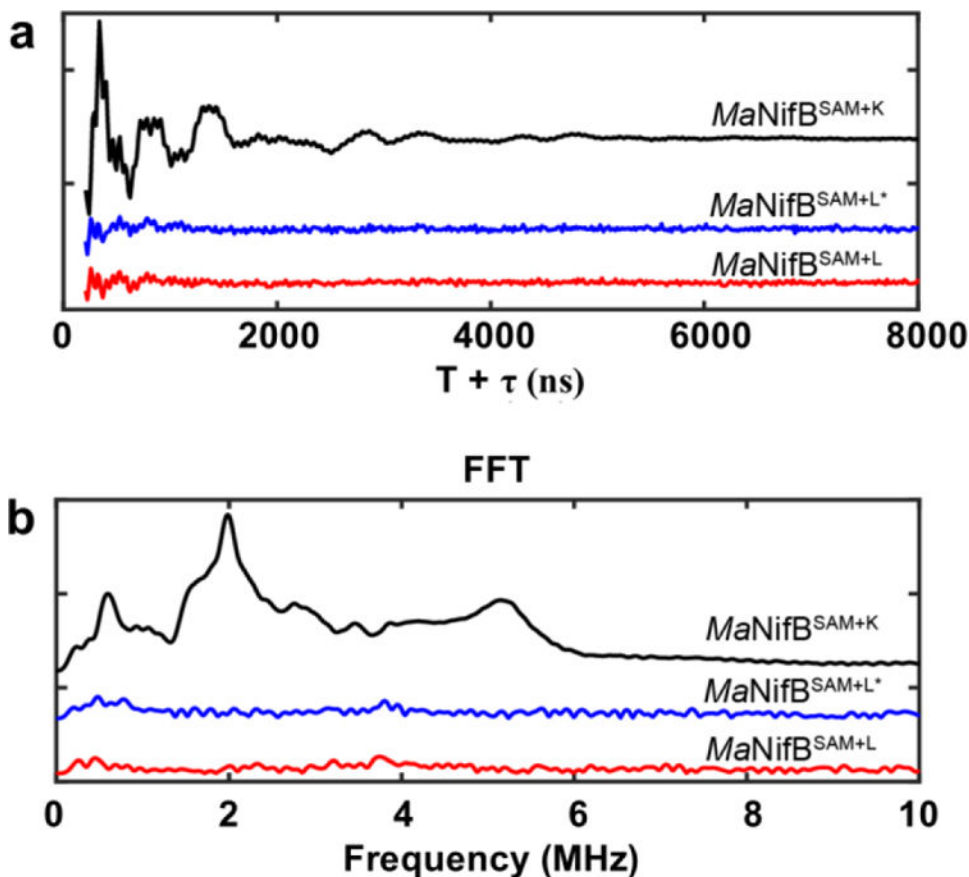
Figure 2.
(**a**) Three-pulse ESEEM spectra and (**b**) FFTs of MaNifB^{SAM+K} (*black*), MaNifB^{SAM+L*} (*blue*) and MaNifB^{SAM+L} (*red*). The large modulations observed in the time trace (A) and the corresponding FFT peaks of MaNifB^{SAM+K} between 0–6 MHz (B) are characteristic of the hyperfine coupling of a nitrogen coordinating the K1 cluster. These modulations from the ligating nitrogen are lost upon L*- and L-cluster formation. Experimental conditions: $\pi/2$ width=12 ns, τ=128 ns, T increments=16 ns, frequency=9.816 GHz, temperature=10 K.
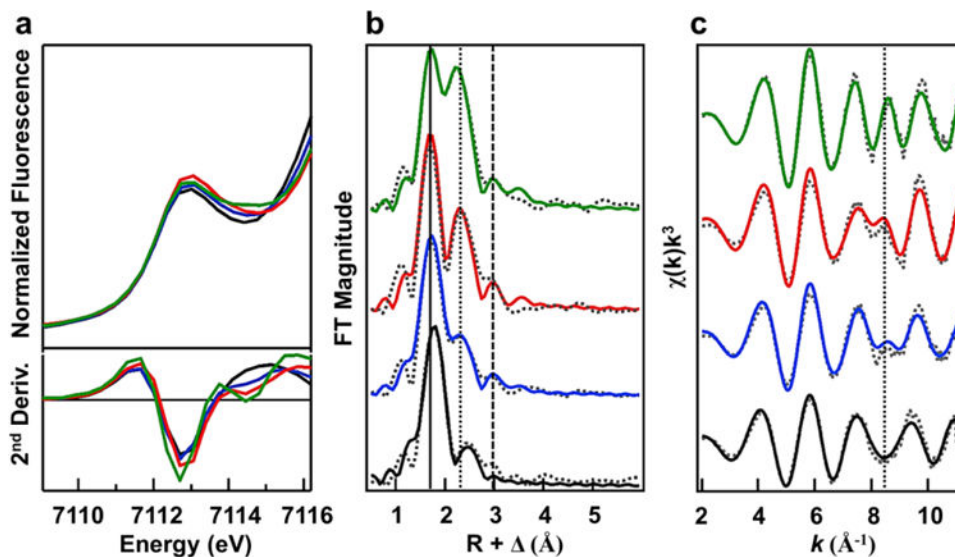
Figure 3.
Fe K-edge XAS analysis of the K- (*black*), L*- (*blue*), L- (*red*) clusters on *Ma*NifB and the L-cluster (*green*) on NifEN. (**a**) Pre-edge region of the normalized fluorescence spectra (*upper*) and smoothed second derivatives of the pre-edge regions (*lower*). (**b**) Fourier transforms of the EXAFS data (*dotted*) and the best fits of data (*solid*). (**c**) k^3-weighted EXAFS data (*dotted*) and the best fits of data (*solid*). See Supporting Information for EXAFS fits (Figures S3–S8; Tables S2–S7; also see Supplementary Discussion, "Best fits of EXAFS data").

Table 1.

Best fits of the Fe K-edge EXAFS data of various precursor species of the M-cluster.

Species	Fe-S			Fe••Fe			Fe••Fe		
	N	R(Å)	σ^2 (10^{-3})	N	R(Å)	σ^2 (10^{-3})	N	R(Å)	σ^2 (10^{-3})
*Ma*NifB-K	3.8	2.29	8.19	1	2.51	5.82	1.5	2.69	4.35
*Ma*NifB-L*	3	2.24	4.95	3	2.62	9.30	1.2	3.69	6.96
*Ma*NifB-L	3.1	2.23	4.23	3.5	2.64	7.87	1.5	3.70	7.89
NifEN-L	3.1	2.25	5.06	3.8	2.64	5.70	1.6	3.72	4.71